Research Article GU J Sci 35(2): 618-629 (2022) DOI: 10.35378/gujs.872959

Gazi University

Journal of Science

http://dergipark.gov.tr/gujs

The Effect of Annealing Technique on ZnO Film Properties

Meryem POLAT GONULLU*

Gazi University, Department of Metallurgical and Materials Engineering, 06500, Ankara, Turkey

Highlights

- This paper focuses on the effect of the annealing technique on ZnO film properties.
- Microwave and standard thermal annealing techniques are applied to the films.
- Improved crystalline properties were determined for microwave annealed ZnO films.

Article Info

Received: 03 Feb 2021
Accepted:11 June 2021

Keywords

ZnO film
Annealing technique
Microwave annealing
Characterization

Abstract

ZnO films deposited on glass substrates by ultrasonically chemical spray pyrolysis technique have been investigated to establish the effect of the annealing technique on film properties. For this purpose, films have been exposed to standard thermal annealing and microwave annealing in an air atmosphere. It has been determined that the structural, morphological, compositional, and optical properties of the ZnO films correlate with each other. X-ray diffraction analyses have been revealed the highest crystallization level and changing preferred orientations for microwave annealed films. It has been identified that the optical band gap values of the films decreased from 3.27 eV to 3.23 eV and 3.21 eV after the standard and microwave thermal annealing, respectively. Scanning electron microscope images have been revealed homogeneous morphology at plan-view images of all films. Also, it has been determined that the root-like morphology from the higher magnification scanning electron microscopy images. Thicknesses of the films have been also determined from cross-sectional scanning electron microscope images as 1.04μm, 0.92 μm, and 0.92 μm for ZnO, standard thermal annealed and microwave annealed ZnO films, respectively. Also, the O/Zn ratio revealed improved stoichiometry for annealed films according to as-deposited film for investigated regions. The dependence of photoluminescence intensity on annealing technique has also been investigated in the current study.

1. INTRODUCTION

Zinc oxide (ZnO) is a member of the group II-VI family with fascinating properties such as wide and direct optical band gap (~3.37 eV), large excitation binding energy (~60 meV) at room temperature, chemical and thermal stability [1-3], etc. As a result of these features, ZnO has gained extensive research potential in technological applications from optoelectronic devices to photocatalysis [4, 5]. Various production methods are applicable for the production of ZnO films including chemical vapor deposition (CVD), physical vapor deposition (PVD), ultrasonically spray pyrolysis (USP), atomic layer deposition (ALD), and sputtering [6-10]. Among these methods, ultrasonically spray pyrolysis provides low cost, large area deposition, ease of use and easy modification facility. Requiring no vacuum is also another advantage of spray pyrolysis. In this technique, the films are deposited by spraying the starting solution onto pre-heated substrates. An ultrasonic atomizer is utilized to atomize starting solution to produce thin or thick films. Different type of substrates can be used for the coating with different geometries. By adjusting the production parameters such as spray nozzle to substrate distance, substrate temperature, starting solution molarity, solution flow rate, and solution solvent type etc. physical properties of spray deposited films can be changed [11,12].

Crystallization of ZnO structures occurs in three forms. These are the hexagonal wurtzite that is the most stable and most common phase, zinc blende that is metastable structure, and rocksalt structure which is transformed from wurtzite structure under high-pressure conditions [13]. Occurring of these structures is related to production methods, process parameters, and substrate type [14-16], etc. In order to improve the

*e-mail: meryempolat@gazi.edu.tr

physical properties of ZnO and increasing potential applications, annealing is an effective approach. For this purpose, many investigations have been made using a variety of annealing conditions such as atmosphere annealing, atmosphere-controlled annealing in nitrogen, argon, and oxygen ambient, and rapid thermal annealing (RTA) [17-21], etc. Besides, the microwave (MW) annealing method which is attracting attention lately in semiconductor-based materials provides advantages with improved crystal properties according to classical methods [22].

In line with this information, this work is focused on the effect of the annealing technique on structural, morphological, compositional, and optical properties of ZnO films produced by the USP technique. Thus, ZnO films have been annealed with standard thermal annealing (STA) and microwave annealing (MW) techniques at 600°C for 1 hour. As-deposited and annealed films have been characterized and resulting film properties have been discussed.

2. EXPERIMENTAL

ZnO films have been deposited on microscope glass substrates by the USP technique at a substrate temperature of 400±5 °C using air as carrier gas with a pressure of 1 atm. The schematic diagram and working principle of the USP technique are given in detail in previous work [23]. The ultrasonic oscillator frequency has been arranged at 100 kHz. The spraying solution has been prepared by dissolving 0.1 M $[(CH_3COO)_2Zn.2H_2O]$ in deionized water to produce ZnO film. Totally 120 cc of the solution has been sprayed onto glass substrates for 30 min. The solution flow rate has been kept at 4 cc min^{-1} and controlled by a flowmeter. After the production, films have been annealed at 600°C for 1 hour by two different annealing techniques which are standard thermal annealing (STA) (PROTHERM) and microwave annealing (MWA) (SYNOTHERM, 800 W) in air atmosphere. The samples are named as Z-As, Z-STA, and Z-MWA according to the as-deposition and annealing technique. Structural analysis of the samples has been performed by Bruker D8 Advanced diffractometer with CuK_α (1.5418 Å) radiation. Surface morphologies, film thicknesses, and the elemental compositions of the films have been investigated by Jeol JSM 6060LV Scanning electron microscope (SEM) equipped with IXRF systems. Optical properties have been analyzed by Shimadzu UV-Visible model 2600 spectrophotometer in the range of 200 nm to 700 nm. The PL spectra have been measured by a Horiba Jobin Yvon Fluorolog-3spectrometer with 325 nm He-Cd laser.

3. RESULT AND DISCUSSION

X-ray diffraction (XRD) patterns of Z-As, Z-STA, and Z-MWA films are shown in Figure 1. It has been determined that the peaks seen from XRD spectra well match with the peaks in the ICDD card: 36-1451. The presence of peaks corresponding to (100), (002), (101), (102), (110), (103), (200), (112), and (201) planes with different intensities (indicated by a line equal to 5000 counts) related to the hexagonal wurtzite crystal structure of ZnO exhibit the polycrystalline nature of the films.

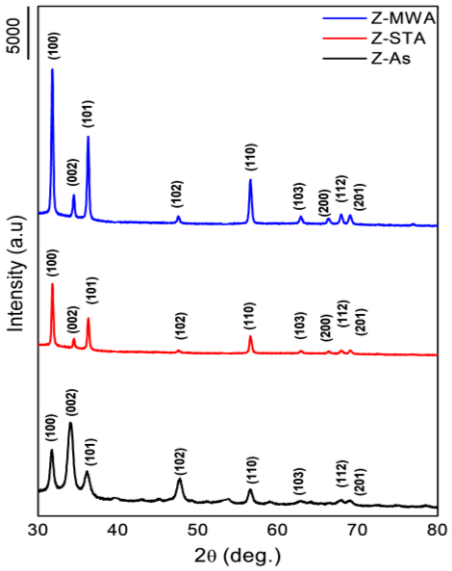

Figure 1. *XRD patterns of Z-As, Z-STA, and Z-MWA films*

Table 1 shows the data related to three major peaks with different intensities and widths on XRD patterns with ICDD (Card No: 36-1451) values. An obvious increase in the diffraction intensity of Z-MWA film reveals the higher crystallinity level after the microwave annealing of ZnO film. Also, shifting in the peak positions and decreasing interplanar spacing to the ICDD values, and decreasing in full width half maximum (β) values are seen for Z-STA and Z-MWA films according to Z-As film.

Table 1. *Data related to three major peaks from XRD patterns with ICDD values*

Sample	Miller Indice	2θ	$2\theta_0$	I	I_0	d	d_0	β
Z-As	(100)	31.701	31.770	6463	58	2.82026	2.81430	0.472
	(002)	34.038	34.422	9159	45	2.63183	2.60332	0.738
	(101)	36.124	36.253	4412	101	2.48444	2.47592	0.638
Z-STA	(100)	31.792	31.770	7365	58	2.81242	2.81430	0.247
	(002)	34.514	34.422	1982	45	2.59659	2.60332	0.236
	(101)	36.283	36.253	4012	101	2.47393	2.47592	0.274
Z-MWA	(100)	31.792	31.770	15963	58	2.81242	2.81430	0.260
	(002)	34.469	34.422	3619	45	2.59991	2.60332	0.253
	(101)	36.261	36.253	9342	101	2.47543	2.47592	0.272

The other structural parameters such as texture coefficient (P), crystallite size (D), dislocation density (δ), and microstrain <e> values have also been evaluated which are given in Table 2 and calculated by following relations [24, 25];

$$P(h_i k_i l_i) = \frac{I(h_i k_i l_i)}{I_o\,(h_i k_i l_i)} \left[\frac{1}{n} \sum_{i=1}^{n} \frac{I(h_i k_i l_i)}{I_o\,(h_i k_i l_i)}\right]^{-1}, \quad (1)$$

$$D = \frac{0.9\,\lambda}{\beta cos\theta}\ , \quad (2)$$

$$\delta = \left(\frac{1}{D}\right)^2, \quad (3)$$

$$\varepsilon = \frac{d - d_o}{d_o}\,. \quad (4)$$

Here, I_o is the standard intensity (ICDD), I is the observed intensity of $(h_i k_i l_i)$ plane, n is the reflection number, β is the half-width of the peak with maximum intensity as radian, D is the crystallite size, λ is the

wavelength of X-ray, θ is the Bragg angle, d is the interplanar spacing and d_o is the interplanar spacing without deformation [24, 25]. Surface tensions, strains between the glass substrate and polycrystalline film, and inner strains as residual stresses in the film have been neglected.

The evaluated structural parameters have also been determined for three intense peaks of the ZnO structure. From the XRD parameters, it has been obtained that Z-As film shows preferential orientation (P) which is highlighted in bold type, through the (002) diffraction plane. Also, an alteration has been determined for preferential orientations of Z-STA and Z-MWA films from (002) to (100) diffraction plane after the thermal annealing. This rearrangement of the crystal orientations has been associated with increasing oxygen ratio in the literature [26, 27]. Also, it can be said that these increased texture coefficient values of the annealed films indicate increasing crystallites.

Table 2. *Calculated structural parameters of ZnO films*

Sample	Miller Indice	P	D(nm)	<e>	δ(line/nm^2)
Z-As	(100)	0.932094	17.518	2.12E-03	3.26E-03
	(002)	**1.702507**	11.271	1.10E-02	7.87E-03
	(101)	0.365399	12.232	3.44E-03	6.68E-03
Z-STA	(100)	**1.807583**	33.484	-6.68E-04	8.92E-04
	(002)	0.626967	35.293	-2.59E-03	8.03E-04
	(101)	0.565449	30.548	-8.04E-04	1.07E-03
Z-MWA	(100)	**1.842437**	31.809	-6.68E-04	9.88E-04
	(002)	0.538372	32.917	-1.31E-03	9.23E-04
	(101)	0.619191	30.771	-1.98E-04	1.06E-03

From Table 2, it can be seen that the crystallite size (D) values of ZnO films have been varied in the range of 11-35 nm. This increase in the crystallite sizes of Z-STA and Z-MWA films indicates the decreasing grain boundaries in the film structure. Also, almost the same crystallite sizes have been determined for annealed films. Dislocation density (δ) values that show the number of dislocation lines per unit volume have been detected minimum for Z-MWA film. The lowest value of dislocation density indicates the decreasing defects in the film structure and increasing film quality for microwave annealed film. Also, negative microstrain values have been obtained for annealed films that indicating the reduction of compressive stresses in the film as defined by Equation (4) according to Z-As. Generally, it can be said that the Z-STA and Z-MWA films have enhanced properties according to Z-As film to the data obtained. However, among the annealed films, Z-MWA film highlights its improved features like highest crystallinity level, 2θ and interplanar d spacing values closest to standard, while Z-STA film has better β and microstrain values that almost the same with Z-MWA film.

The surface images of Z-As, Z-STA, and Z-MWA films have been taken by SEM at X30 magnification plan-view, X1000, and X3000 (inset image) magnification in detail and given in Figure 2. Smooth surface properties have been obtained for all films from the SEM images taken at X30 magnification that indicate the uniform deposition on the substrate surface. The micrographs taken at X1000 magnification presents the detailed surface morphology of ZnO films with droplet trails related to spraying. Also, root-like areas are seen in these images and given in inset images taken at X3000 magnification, in detail. An increasing trend has been determined in the root-like morphology of the Z-STA and Z-MWA films that are may be related to the relaxation of stress in the structure of the films as a result of annealing. Xu Li et al. [28], explain this formation with the effect of annealing process while H. Sutanto et al. [29], explain it with temperature difference between the first and other layers which causes the merging particles to make a long ZnO structure. K. Navin et al. [30], also clarify this phenomenon by changing the decomposition rate of precursor solutions and evaporation of the solvent by changing the heating rate. S.J Kwon et al. [31], also reported formation of root-like network morphology which is caused by the relaxation of stress as a result of the evaporation of solvent. Another possible mechanism has been explained by Scherer et al. [32], as loss of hydroxyl/alkoxy group by heating process for the production of these formations. In this study, this

root-like type formation is thought to be in a relationship with the relaxation of stress after annealing besides evaporation of precursor solution during the production process on heated substrates.

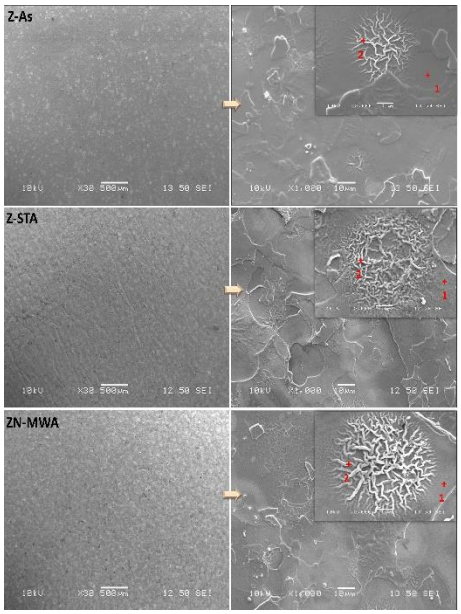

Figure 2. *SEM images of Z-As, Z-STA, and Z-MWA films*

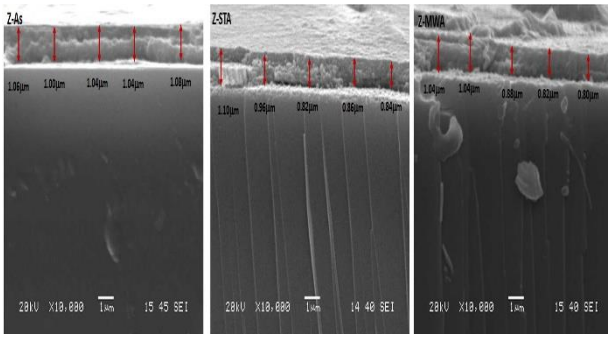

Figure 3. *Cross-sectional SEM images of Z-As, Z-STA, and Z-MWA films with their thicknesses that obtained five different location*

Thicknesses of the films have been obtained by cross-sectional SEM images that are given in Figure 3. From these figures, average thickness of Z-As film has been obtained as 1.04 μm. After the annealing at different conditions, it has been determined that the thicknesses of the Z-STA and Z-MWA changed to 0.92 nm for both films. This decreasing in the thicknesses could be attributed to the transforming of the films to the more ordered phases, reduced defects, and dimensional changes. This situation also could be explained by desorption of atoms by substrate surface as a result of increasing temperature with the effect of annealing.

Energy dispersive X-Ray spectroscopy (EDX) has been used to obtain detailed information about film compositions. In Figure 4, only the spectra of the plan-view images have been presented in order to avoid visual confusion due to the similarity of EDX spectra to each other. In these spectra, the presence of zinc, oxygen, and silicon (comes from the glass substrate and neglected) elements are observed. Also, elemental compositions have been individually investigated on the plan-view, matrix (marked as 1), and root-like (marked as 2) regions to exhibit the distribution of the oxygen and zinc elements in the different regions of whole structure. Atomic weights (at%) of Zn and O elements and O/Zn ratio from these regions are listed in Table 3.

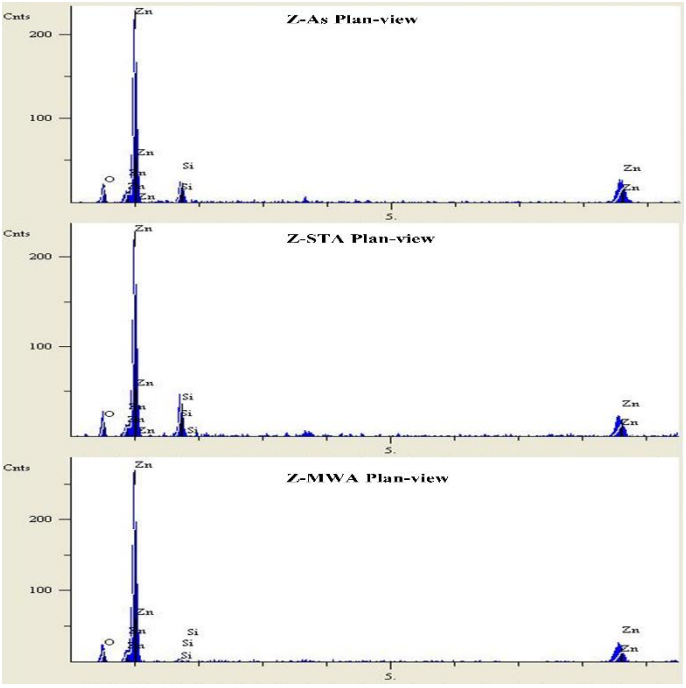

Figure 4. *EDX spectra of Z-As, Z-STA, and Z-MWA films from the plan-view*

Table 3. *Elemental compositions and O/Zn ratio of ZnO films*

Sample	Selected Area	O at%	Zn at%	O/Zn ratio
Z-As	Plain-view	42.498	57.502	0.739
	Matrix	28.676	71.324	0.402
	Root-like	38.820	61.180	0.635
Z-STA	Plain-view	49.538	50.462	0.982
	Matrix	38.536	61.464	0.627
	Root-like	45.127	54.873	0.822
Z-MWA	Plain-view	45.989	54.011	0.851
	Matrix	42.869	57.131	0.750
	Root-like	43.915	56.085	0.783

Compositional distributions of O and Zn elements obtained from plan-view images (X30) that give the data from the larger area of the films present the increasing film stoichiometry. This is may be attributed to the oxidation of the Z-STA and Z-MWA films after the annealing under the air atmosphere. Also, Z-STA film presents the higher stoichiometry from the plan-view analysis in all films. Detailed investigations evaluated on the matrix and root-like formations given in the inset images at X3000 magnification present the Z-As film has excess Zn element for all regions that indicates the non-uniform distributions of the elements. Besides, annealed films indicate the improved and more homogeneous distribution of oxygen and zinc elements in their structures. Although the Z-STA film exhibits improved stoichiometry from the plan-view analysis, it can be seen from Table 3 that the Z-MWA film has higher homogeneity between the matrix and root-like regions that indicates the better distribution of elements in its structure. This is another proof that the evaporation of the precursor solution during the production process and annealing in the oxygen atmosphere improves the compositions of the films.

Absorbance spectra of the as-deposited and annealed ZnO films are shown in Figure 5.

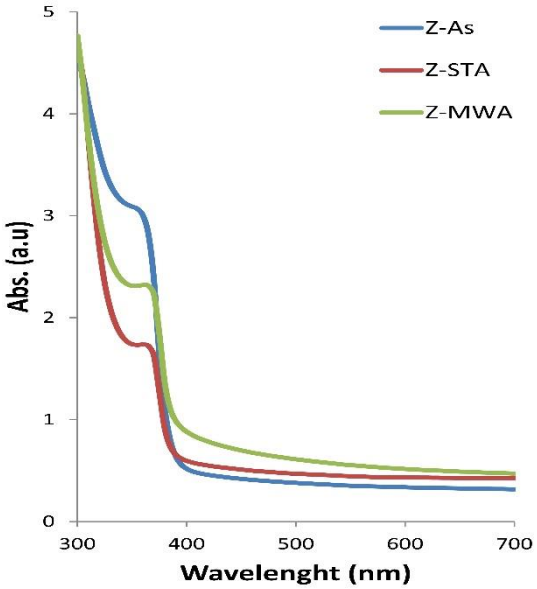

Figure 5. *Absorbance spectra of Z-As, Z-STA, and Z-MWA films*

Fundamental absorption edges have been observed at almost similar wavelengths from the absorption spectra of the films. Using these absorption spectra of the films, $(\alpha h\nu)^2$ - $(h\nu)$ plots have been obtained and optical band gap values of the ZnO films have been determined by optical method which is given in Figure 6. As a result, it has been determined that as-deposited and annealed films have direct band gap transitions. The optical band gap values have been obtained as 3.27, 3.23, and 3.21 eV for Z-As, Z-STA, and Z-MWA films, respectively. Also, decreased band gap values according to bulk ZnO have been determined for annealed films that could be associated with improved crystal properties. Especially, a distinct decreasing has been obtained for optical band gap values of Z-MWA film from 3.27 to 3.21 eV. In the earlier reports, J. Gonioakowski and C. Noguera have been explained this situation with the various lattice associated atomic interaction phenomena occurring from ionic crystalline lattice nature of ZnO. Caglar et. al,, Sengupta et. al., and Ghosh et. al. have also identified this with increasing crystallinity as a result of reducing defects and stress as seen in the XRD result of this study [33-36]. This band gap narrowing of the absorption edge toward higher wavelengths allows for visible light driven photocatalytic applications [37].

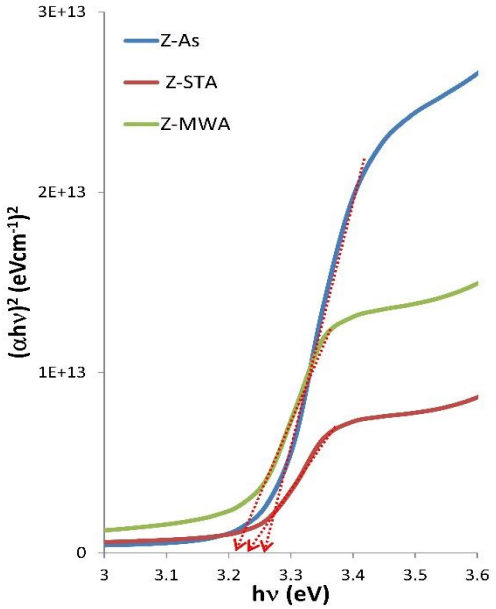

Figure 6. *$(\alpha h\nu)^2$ - $(h\nu)$ plots of Z-As, Z-STA, and Z-MWA films*

The room temperature photoluminescence (PL) spectra of the as-deposited and annealed ZnO films on glass substrate with a 325 nm excitation wavelength have been illustrated in Figure 7. From the spectra, it can be seen that the numbers, positions, and intensities of the PL peaks are affected by annealing. For Z-As film, the PL spectrum consists of two emission bands that indicate the strong UV emission band at ~390 nm (3.18 eV), and weak green emission band ~514 nm (2.41 eV), respectively. The band emission emerging in the UV range is due to the excitonic recombination, while the band emissions existing at the visible range are due to the recombination of deep-level holes and electrons [38]. It is known from the literature that these deep level emissions are related to the point defects occurring during the production of crystallites and/or related to the change of crystallinity due to the zinc interstitials (Zn_i), zinc vacancies (Zn_v), oxygen interstitials (O_i), oxygen vacancies (O_v), and dislocations [39]. After the annealing of ZnO films by two different techniques, it has been observed that the intensity of the UV emission band decreased abruptly and shifted to lower wavelengths (blue shift). This shifting is stated in the literature that the change of stress along the lattice distortion in accordance with the XRD analysis [40]. On the other hand, new strong and narrow emissions have been determined for Z-STA and Z-MW films in the visible range of the spectrum ~503 nm, ~528 nm (green emission bands), ~662 nm and ~ 650 nm (orange-red emission bands), respectively. Increasing in the visible emissions (green and/or orange-red emissions) of ZnO have been associated with the oxygen defects like excess oxygen concentrations and oxygen interstitials by the effect of annealing in oxygen ambient in the literature [41-44].

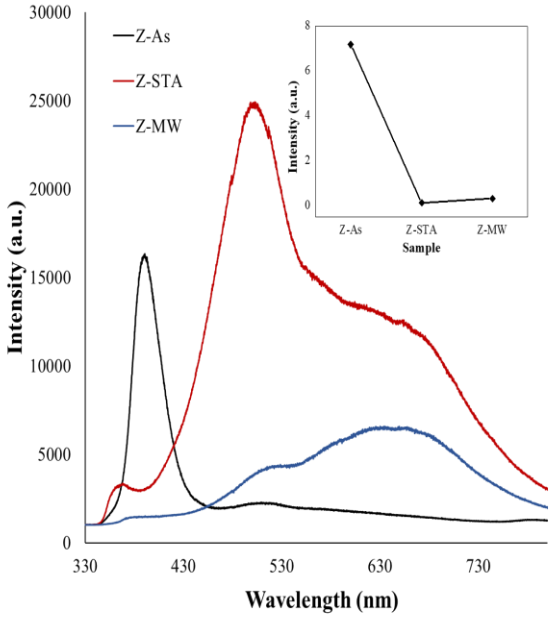

Figure 7. *Absorbance spectra of Z-As, Z-STA, and Z-MWA films*

The inset of Figure 7 shows the UV to green emission peak ratios as a function of annealing techniques. The intensity ratio of UV to green emission peaks has been determined as 7.18, 0.14, and 0.33 for Z-As, Z-STA, and Z-MW films, respectively. Decreasing in this ratios for annealed films indicates the increasing amount of point defects in the ZnO film. However, an increase more than 2 times has been observed for the intensity ratios of Z-MW according to Z-STA film. This indicates the microwave annealing is more effective at producing a less defective structure and/or in reducing point defects in the ZnO film structure. Although the point defects in the material structure are generally expected to decrease as a result of the annealing process, in the current study the increase in the point defects is thought to be due to rearrangements of crystal structure/phase transitions between the (002) to (100) diffraction planes as seen in the XRD analysis.

4. CONCLUSION

In this work, the effect of the annealing technique on the properties of ZnO films has been investigated. ZnO films have been deposited on glass substrates by Ultrasonic Spray Pyrolysis Technique. Then two different techniques which are STA and MWA techniques have been applied for thermal annealing. X-ray diffraction analyzes have been shown improved crystallinity levels for annealed films, especially that microwave annealing. After the annealing, alterations in the preferential orientations of ZnO films have been observed from (002) to (100) diffraction planes. Microstrain and dislocation density values of ZnO films reduced after the annealing of ZnO films with both annealing techniques. Root-like morphology has been detected when looking at the smooth and homogeneous surface of the films in detail at higher magnifications. An increase in this root-like morphology has been observed, resulting in an interconnected network structure. Increased O/Zn ratios obtained for annealed films from all investigated regions indicate the improved elemental distribution in the film structure. Annealed films have been exhibited a decrease in the optical band gaps according to Z-As film from 3.27eV to 3.23 eV, and 3.21 eV, respectively. PL spectra of the films have been presented the point defect behavior in the structure of the films after the annealing and indicated the microwave annealing decreases the oxygen related point defect density according to standard thermal annealing technique. In annealed films, while Z-STA film presents the better stoichiometry on plan-view, and lower microstains and higher crystallite size in the crystal structure, Z-MWA film draw attention with the properties of higher crystalline level, lower dislocation and point defect densities, crystal properties closest to standard, and lower optical band gap values. So, it can be said that microwave annealing is a more suitable technique for producing higher quality ZnO films for many applications like higher crystal quality optical materials used in photocatalysis.

CONFLICTS OF INTEREST

No conflict of interest was declared by the author.

REFERENCES

[1] Pearton, S. J., Norton, D. P., Ip, K., Heo, Y. W., Steiner, T., "Recent progress in processing and properties of ZnO", Progress in Materials Science, 50: 293-340, (2005).

[2] Triboulet, R., and Perrière, J., "Epitaxial growth of ZnO films", Progress in Crystal Growth and Characterization of Materials, 47(2-3): 65-138, (2003).

[3] Hoffman R. L, Norris, B. J., Wager, J. F., "ZnO-based transparent thin film transistors", Applied Physics Letters, 82(5): 733-735, (2003).

[4] Willander, M., Nur O., Zhao, Q., Yang, L., Lorenz, M., Cao, B., Žiga Pérez, J., Czekalla, C., Zimmermann, G., Grundmann, M., Bakin, A., Behrends, A., Al-Suleiman, M., El-Shaer, A., Che Mofor, A., Postels, B., Waag, A., Boukos, N., Travlos, A., Kwack, H., Guinard, J., Le Si Dang, D., "Zinc oxide nanorod based photonic devices: Recent progress in growth, lightemitting diodes and lasers", Nanotechnology, 20(33): 332001, (2009).

[5] Di Mauro, A., Fragalà, M. E., Privitera, V., Impellizzeri, G., "ZnO for application in photocatalysis: From thin films to nanostructures", Materials Science in Semiconductor Processing, 69: 44-51 (2017).

[6] Purica, M., Budianu, E., Rusu, E., Danila, M., Gavrila, R., Optical and structural investigation of ZnO thin films prepared by chemical vapor deposition (CVD)", Thin Solid Films, 403: 485-488, (2002).

[7] Wang, L., Zhang, X., Zhao, S., Zhou, G., Zhou, Y., Qi, J., "Synthesis of well-aligned ZnO nanowires by simple physical vapor deposition on c-oriented ZnO thin films without catalysts or additives," Applied Physics Letters, 86(2): 024108, (2005).

[8] Bilgin, V., Kose, S., Atay, F., Akyuz, I., "The effect of Sn concentration on some physical properties of zinc oxide films prepared by ultrasonic spray pyrolysis", Journal of Materials Science, 40(8): 1909-1915, (2005).

[9] Gonullu, M. P., and Ates, H., "Atomik Katman Biriktirme Tekniğine Genel Bakış: ZnO, TiO_2 ve Al_2O_3 Filmlerin Üretimi", Gazi Üniversitesi Fen Bilimleri Dergisi Bölüm C: Tasarım ve Teknoloji, 7(3): 649-660, (2019).

[10] Gao W., and Li, Z., "ZnO thin films produced by magnetron sputtering", Ceramics International, 30(7): 1155-1159, (2003).

[11] Perednis, D., and Gauckler, L. J., "Thin film deposition using spray pyrolysis", Journal of Electroceramics, 14(2): 103-111, (2005).

[12] Patil, P. S., "Versatility of chemical spray pyrolysis technique", Materials Chemistry and Physics, 59(3): 185-198, (1999).

[13] Bates, C. H., White, W. B., Roy, R., "New High-Pressure Polymorph of Zinc Oxide", Science, 137: 993, (1962).

[14] Garnier, J., Bouteville, A., Hamilton, J., Pemble, M. E., Povey, I. M., "A comparison of different spray chemical vapour deposition methods for the production of undoped ZnO thin films", Thin Solid Films, 518(4): 1129-1135, (2009).

[15] Bacaksiz, E., Parlak, M., Tomakin, M., Özçelik, A., Karakiz, M., Altunbaş, M., "The effects of zinc nitrate, zinc acetate and zinc chloride precursors on investigation of structural and optical properties of ZnO thin films", Journal of Alloys and Compounds, 466(1-2): 447-450, (2008).

[16] Yoon S. H., and Kim, D. J., "Effect of substrate on the preferred orientation of ZnO films by chemical solution deposition", Journal of Crystal Growth, 303(2): 568-573, (2007).

[17] Salameh, B., Alsmadi, A. M., Shatnawi, M., "Effects of Co concentration and annealing on the magnetic properties of Co-doped ZnO films: Role of oxygen vacancies on the ferromagnetic ordering", Journal of Alloys and Compounds, 835: 155287, (2020).

[18] Chu, C. H., Wu, H. W., Huang, J. L., "Effect of annealing temperature and atmosphere on aluminum-doped ZnO/Au/aluminum-doped ZnO thin film properties", Thin Solid Films, 605: 121-128, (2016).

[19] Goktas, A., "High-quality solution-based Co and Cu co-doped ZnO nanocrystalline thin films: Comparison of the effects of air and argon annealing environments", Journal of Alloys and Compounds, 735: 2038-2045, (2018).

[20] Cui, L., Zhang, H. Y., Wang, G. G., Yang, F. X., Kuang, X. P., Sun, R., Han, J. C., "Effect of annealing temperature and annealing atmosphere on the structure and optical properties of ZnO thin films on sapphire (0001) substrates by magnetron sputtering," Applied Surface Science, 258(7): 2479-2485, (2012).

[21] Xue, X. T., Gu, Y., Ma, H. P., Hang, C. Z., Tao, J. J., Lu, H. L., Zhang, D. W "Effect of rapid thermal annealing on the properties of zinc tin oxide films prepared by plasma-enhanced atomic layer deposition", Ceramics International, 46(9): 13033-13039, (2020).

[22] Kuşkonmaz N. and Kutbay, I., "Mikrodalga ısıtmanın seramik üretiminde kullanımı," Metalurji Dergisi, 137: 52-56, (2004).

[23] Atay, F., V, Bilgin., Akyuz, I., Kose, S.,"The effect of in doping on some physical properties of CdS films", Materials Science in Semiconductor Processing, 6: 197-203, (2003).

[24] Barrett, C. S., and Massalski, T.B., Structure of Metals, 35, Third edition, Pergamon, Oxford, New York, 204, (1980).

[25] Bilgin, V., Akyuz, I., Ketenci, E., Kose, S., Atay, F., "Electrical, structural and surface properties of fluorine doped tin oxide films", Applied Surface Science, 256(22): 6586-6591, (2010).

[26] Abdallah, B., Jazmati, A. K., Refaai, R., "Oxygen effect on structural and optical properties of ZnO thin films deposited by RF magnetron sputtering", Materials Research, 20(3): 607-612, (2017).

[27] Yue-Hui, H., Yi-Chuan, C., Hai-Jun, X., Hao, G., Wei-Hui, J., Fei, H., Yan-Xiang, W. "Texture ZnO thin-films and their application as front electrode in solar cells", Engineering, 2: 973-978, (2010).

[28] Xu, Li., Zhu, X., Yang, D., "Enhanced luminescent performance with surface wrinkled Al-doped ZnO films", Journal of Materials Science: Materials in Electronics, 31: 6304-6312, (2020).

[29] Sutanto, H., Durri, S., Wibowo, S., Hadiyanto, H., Hidayanto, E., "Rootlike morphology of ZnO:Al thin film deposited on amorphous glass substrate by sol-gel method", Physics Research International, 2016: 1-7, (2016).

[30] Navin, K. and Kurchania, R., "Structural, Morphological and Optical Studies of Ripple-Structured ZnO Thin Films", Applied Physics A: Materials Science and Processing, 121: 1155-1161, (2015).

[31] Kwon, S. J. Park, J. H., Park, J. G., "Wrinkling of sol–gel-derived thin Film", Physical Review E 71: 011604, (2005).

[32] Scherer, G. W., "Sintering of sol–gel films", Journal of Sol-Gel Science and Technology 8(1): 353-363, (1997).

[33] Goniakowski, J., and Noguera, C., "Relaxation and rumpling mechanisms on oxide surfaces", Surface Science, 323(1-2): 129-141, (1995).

[34] Caglar, Y., Ilican, S., Caglar, M., Yakuphanoglu, F., "Effects of In, Al and Sn dopants on the structural and optical properties of ZnO thin films", Spectrochimica Acta Part A: Molecular and Biomolecular Spectroscopy, 67(3-4): 1113-1119, (2007).

[35] Sengupta, J., Sahoo, R. K., Bardhan, K. K., Mukherjee, C. D., "Influence of annealing temperature on the structural, topographical and optical properties of sol–gel derived ZnO thin films", Materials Letters, 65(17-18): 2572-2574, (2011).

[36] Ghosh, R., Basak, D., Fujihara, S., "Effect of substrate-induced strain on the structural, electrical, and optical properties of polycrystalline ZnO thin films", Journal of Applied Physics, 96(5): 2689-2692, (2004).

[37] Ramírez-Ortega D., Meléndez, A. M., Acevedo-Peña, P., González, I., Arroyo, R., "Semiconducting properties of ZnO/TiO_2 composites by electrochemical measurements and their relationship with photocatalytic activity", Electrochimica Acta, 140: 541-549, (2014).

[38] Hong, R., Qi, H., Huang, J., He, H., Fan, Z., & Shao, J., "Influence of oxygen partial pressure on the structure and photoluminescence of direct current reactive magnetron sputtering ZnO thin films", Thin Solid Films, 473(1): 58-62, (2005).

[39] Djurišić, A. B., Choy, W. C., Roy, V. A. L., Leung, Y. H., Kwong, C. Y., Cheah, K. W., Gundu Rao, T. K., Chan, W. K., Fei Lui, H., Surya, C., "Photoluminescence and electron paramagnetic resonance of ZnOtetrapod structures", Advanced Functional Materials, 14(9): 856–864, (2004).

[40] Nehru, L. C., Umadevi, M., Sanjeeviraja, C., "Studies on structural, optical and electrical properties of ZnO thin films prepared by the spray pyrolysis method". International Journal of Materials Engineering, 2(1): 12-17, (2012).

[41] Djurišić, A. B., Leung, Y. H., Tam, K. H., Hsu, Y. F., Ding, L., Ge, W. K., Zhong, Y. C., Wong, K. S., Chan, W. K., Tam, H. L., Cheah, K. W., Kwok, W. M., Phillips, D. L., "Defect emissions in ZnO nanostructures", Nanotechnology, 18(9): 095702(8pp), (2007).

[42] Zhang, X., Qin, J., Xue, Y., Yu, P., Zhang, B., Wang, L., Liu, R., "Effect of aspect ratio and surface defects on the photocatalytic activity of ZnO nanorods", Scientific reports, 4(1): 1-8, (2014).

[43] Peng, W. Q., Qu, S. C., Cong, G.W., Wang, Z. G., "Structure and visible luminescence of ZnO nanoparticles", Materials Science in Semiconductor Processing, 9(1–3): 156–159, (2006).

[44] Panigrahy, B., Aslam, M., Misra, D. S., Ghosh, M., Bahadur, D., "Defect-related emission and magnetization properties of ZnO Nanorods", Advanced Functional Materials, 20(7): 1161–1165, (2010).